PAPER

Check for updates

Uncovering gamma-stable organic semiconductors: large-scale screening and predictive modelling for radiation-hard applications

Andreas J. Bornschlegl, [ID] *[a] Attila J. Mozer, [ID] *[b] Jessie A. Posar,[c] Jianchang Wu,[ad] Juan S. Rocha-Ortiz, [ID] [ad] Patrick Duchstein, [ID] [e] Mauricio Caicedo-Reina,[f] Alejandro Ortiz, [ID] [fg] Braulio Insuasty, [ID] [fg] Dirk Zahn, [ID] [e] Justin B. Davies,[h] Marco Petasecca,[c] Larry Lüer*[adi] and Christoph J. Brabec*[adij]

Molecular semiconductors have the potential to enable new possibilities in the fields of radiation detection and space applications, but they need to prove resilience against the ionizing radiation present in these harsh environments. The lack of molecular oxygen in space requires the challenging task of performing the degradation studies at inert conditions. In this work, a strategy is presented to investigate the inert radiation hardness of molecular semiconductors using total ionizing dose (TID) tests based on gamma radiation from a cobalt-60 (Co-60) source - a traditional proxy for the space environment. For the first time, a large-scale gamma stability screening of 46 structurally diverse organic semiconductors was performed at inert conditions, deriving a stability target from the UV-visible (UV-vis) evolutions during degradation. The resulting stability ranking of the small-molecule hole transport materials (HTMs) designed for use in perovskite solar cells spans more than two orders of magnitude and shows that molecular structure - rather than atomic composition alone - governs gamma stability. On average, the ionizing dose tolerance exceeds 10 kGy, corresponding to a calculated lifetime of over two years in the Van Allen belt at ~1000 km altitude in low Earth orbit (LEO). Derivatives of 4,4-difluoro-4-bora-3a,4a-diaza-*s*-indacene (BODIPY) stand out, even showing seemingly infinite stability targets. Using the ranking, a predictive model could be trained, which implies that the number of boron atoms – or the BODIPY unit in which they are embedded – outperforms more than 1900 other structural and semi-empirical descriptors. Overall, this work lays the groundwork for future gamma stability studies of molecular semiconductors and thin-film technologies in general. With more efforts targeted at understanding the structure-stability relationships and structure-dependent degradation mechanisms, including up to complete recovery of the UV-vis spectra, this class of materials could become a competitive option for ionizing radiation detectors as well as for organic and perovskite space solar cells.

[a] _Institute of Materials for Electronics and Energy Technology (i-MEET), Department of Materials Science and Engineering, Friedrich-Alexander-Universität Erlangen-Nürnberg (FAU), Martensstraße 7, 91058 Erlangen, Germany. E-mail: andreas.bornschlegl@fau.de, larry.lueer@fau.de, christoph.brabec@fau.de_

[b] _Intelligent Polymer Research Institute and ARC Centre of Excellence for Electromaterials Science, University of Wollongong, Wollongong, New South Wales 2522, Australia. E-mail: attila@uow.edu.au_

[c] _Centre for Medical Radiation Physics, University of Wollongong, Wollongong, NSW, 2522, Australia_

[d] _Helmholtz-Institute Erlangen-Nürnberg for Renewable Energy (HI ERN), Forschungszentrum Jülich GmbH, Immerwahrstraße 2, 91058 Erlangen, Germany_

[e] _Chair for Theoretical Chemistry/Computer Chemistry Center (CCC), Department of Chemistry and Pharmacy, Friedrich-Alexander-Universität Erlangen-Nürnberg (FAU), Nägelsbachstraße 25, 91052 Erlangen, Germany_

[f] _Heterocyclic Compounds Research Group, Department of Chemistry, Universidad del Valle, Calle 13 #100-00, 25360, Cali, Colombia_

[g] _Center for Research and Innovation in Bioinformatics and Photonics-CIBioFi, Calle 13 #100-00, Edificio E-20, No. 1069, 25360, Cali, Colombia_

[h] _Australian Nuclear Science and Technology Organisation, Lucas Heights, Australia_

[i] _FAU Profile Center Solar, Friedrich-Alexander University Erlangen-Nürnberg, Erlangen, Germany_

[j] _IMD-3 Photovoltaics, Forschungszentrum Jülich GmbH, 52428 Jülich, Germany_

This journal is © The Royal Society of Chemistry 2026

Energy Environ. Sci., 2026, **19**, 635–647 | **635**

Broader context

An exponential rise in space satellite deployment and an increasing demand for ionizing radiation detectors in medicine, driven by an aging world population, motivate the development of radiation-hard materials. Organic semiconductors can greatly benefit these fields, enabling straightforward dose-in-tissue conversion due to their tissue equivalence and reduced space launch costs given their low weight. Solution processability even allows printing of solar cells in space, enabling flexible power generation and reduced storage volume. To leverage these properties, organic materials must prove resilient to harsh radiation environments, often tested using Co-60 gamma radiation as a proxy. Most existing studies report strong degradation but cite oxygen and solvent exposure as underlying reasons, conditions unrepresentative of space. Our work addresses this by demonstrating an inert gamma degradation workflow that mimics the oxygen- and water-free space environment, screening 46 molecular semiconductors. Unexpectedly, the stability spans two orders of magnitude, with BODIPY derivatives showing calculated lifetimes corresponding to over 64 years in the Van Allen belt at ~1000 km in LEO. Using a data science approach combining molecular descriptors with a stability target, we developed the first predictive model for gamma stability, which may ultimately enable the inverse design of organic semiconductors for future space applications.

Introduction

The development of radiation-hard materials for space and terrestrial applications is rapidly becoming more relevant. In 2025, more than 9000 functioning space satellites are orbiting the Earth – three times as many as in 2020.[1,2] Given the exponential rise of satellite deployment, a projected tripling of the space economy by 2035 and more countries dramatically expanding their space programs, a high current and future interest in radiation-hard materials for space is certain.[3] Similar demand can be expected in the field of ionizing radiation detection, warranted by over 10 million patients needing radiation therapy each year,[4] increasing use of medical imaging due to an aging world population,[5] and hundreds of nuclear power plants in operation world-wide.[6] The unique properties of organic molecules make this class of materials highly interesting for both fields. Their flexibility and tissue equivalence allow for wearable and even *in vivo* radiation detectors whose sensitivity and selectivity can be tuned *via* molecular design.[7–9] Furthermore, their low weight has the potential to decrease the cost of space launches ($1400 per kg payload)[3] tremendously: currently, organic solar cells can achieve specific powers of well above 30 W g^{-1},[10,11] much higher than that of the typically employed silicon solar modules (0.38 W g^{-1}).[12] Although their areal power density is still lower, they already appear well suited for 1–20 W CubeSats.[13] Furthermore, the solution-processability of organic semiconductors even makes printing of solar cells in space possible, enabling flexible power generation and reduced storage volume.[14] Much of the same applies to perovskite space solar cells, where organic materials are commonly employed in the transport layers, highlighting their importance for both emerging solar cell technologies.[15–18] The crucial question left to answer is whether organic semiconductors can endure the harsh radiation conditions found in space and specialized terrestrial applications. Long since, TID testing based on gamma radiation from the radioactive decay of Co-60 isotopes – emitting photons at 1.17 MeV and 1.33 MeV – has been used as a proxy for harsh radiation environments such as space.[19,20] Due to their high energy, the gamma photons are able to generate a large plethora of ionizing radiation, covering an energy range of 6 orders of magnitude: most importantly, fast electrons (keV–MeV) are produced by ionizing atoms *via* Compton scattering, as well as dense cascades of secondary electrons (eV–keV) created along the tracks of the former. The fast electrons have the potential to displace atoms, replicating the

effects of particle bombardment.[21] Therefore, correlations with electron and even proton bombardment can be drawn, rendering gamma studies a well-rounded method for radiation hardness tests.[22–27] Still, ionization far outweighs displacement and therefore, gamma degradation cannot replace precisely controlled single-event electron or proton bombardment experiments, which are the most commonly employed methods in the latest radiation hardness studies of organic and perovskite solar cells.[28–35] However, a recent publication by Zhang *et al.*, showing a catastrophic 48% PCE decrease of perovskite solar cells after only 0.75 kGy of Co-60 radiation highlights the importance of including gamma studies in the arsenal of radiation hardness tests to achieve future organic and perovskite solar cells with a universal radiation stability in space.[36] For context, radiation-hard electronic components are standardized to withstand a total ionizing dose of more than 1 kGy,[37] with unshielded devices in LEO receiving an annual dose of around 1 kGy to 5 kGy.[38] In contrast to inorganics, organic materials have the natural advantage of having low atomic Z numbers corresponding to low absorption cross sections for electromagnetic radiation, *i.e.*, they absorb negligible amounts of incoming gamma photons and are therefore primarily subjected to the ionizing secondary electrons of extra-cameral material.[39] Coupled with a recent finding that small organic molecules offer high resilience against particle bombardment,[29] it makes this class of materials a promising candidate to study for its radiation hardness. For more than 30 years, many gamma degradation studies on organic semiconductors using Co-60 and Caesium-137 sources have already been performed.[40,41] Investigating representative materials like pentacene,[42] poly[2-methoxy-5-(2′-ethylhexyloxy)-1,4-phenylene vinylene] (MEH-PPV),[43] poly(3,4-ethylenedioxythiophene) polystyrene sulfonate (PEDOT:PSS),[44] poly(3-hexylthiophene-2,5-diyl) (P3HT) and [6,6] phenyl-C61-butyric acid methyl ester (PCBM),[45–48] they showed or proposed highly detrimental effects like chain scission, doping, cross-linking and the formation of radicals, defects and polarons. However, the great majority of gamma degradation studies share that the aging was performed in an ambient environment or in solution, with the studies citing that the solvent or oxygen plays a tremendous role in the degradation.[43,47,49–51] The latter is in line with the findings of photooxidation experiments performed in, *e.g.*, the field of organic solar cells.[52,53] Therefore, the interaction of gamma radiation with the environment instead of the material itself might be the origin of the degradation effects.[54,55] In

636 | *Energy Environ. Sci.*, 2026, **19**, 635–647

This journal is © The Royal Society of Chemistry 2026

reality, the concentration of molecular oxygen in space is negligibly low,[56–58] so studying aging in an inert atmosphere is closer to the space environment. Furthermore, terrestrial radiation detectors could be encapsulated to prevent oxygen from entering the devices. Although literature on gamma degradation in an inert atmosphere is very scarce, the few studies that have been published so far are promising. Park *et al.* showed that doping of P3HT no longer occurs when keeping out oxygen,[46] Martynov *et al.* demonstrated a stable organic solar cell at a gamma dose of up to 6500 Gy,[59] and Freissinet *et al.* reported that all of their five organic materials intended for mass spectrometry equipment in space maintained their full effectiveness after exposure to 3000 Gy, corresponding to the dose rating requirement for a mission to Jupiter's moon Europa.[22] These positive results highlight that there are mechanistic differences between gamma radiation at ambient *vs.* inert conditions and that high stabilities in an inert environment are possible, warranting further studies. One very important investigation is how a wide range of organic semiconductors of different structures and functionalization perform under gamma radiation at inert conditions. Are there structure-stability relationships to consider when selecting materials for radiation-hard applications, or do all materials exhibit similar stability given the small variation in atomic numbers/absorption cross-sections? What makes such investigations challenging and the potential reason why literature is scarce so far, is that the encapsulation needed for the endeavor must both withstand the highly damaging gamma radiation and not interfere with the characterization of the sample.

In the present work, a viable workflow is presented to study the gamma stability of materials in inert conditions, opening the door for future investigations. For this demonstration, 46 state-of-the-art small-molecule HTMs – including materials from an inverse design study achieving perovskite solar cells with 26.2% PCE – were chosen.[60–64] In the inert gamma tests, these structurally diverse organic semiconductors show stabilities ranging over more than 2 orders of magnitude – corresponding to calculated lifetimes of 3 months to more than 64 years in the Van Allen belt at an altitude of ~1000 km in LEO – emphasizing that molecular design is crucial for achieving long lifetimes. One outstanding moiety is BODIPY, even showing up to seemingly infinite values for the employed optical stability target. Furthermore, differential absorbance spectra reveal that varying degradation mechanisms occur – including up to complete recovery of the UV-vis spectra after degradation – depending on the molecular structure, highlighting the gaps in knowledge to be investigated for the development of radiation-hard organic semiconductors used in, *e.g.*, organic and perovskite space solar cells.

Results

To investigate the effect of ionizing gamma radiation on molecular semiconductors in an inert atmosphere, a library of 46 conjugated molecules was chosen and irradiated with a Co-60 source (1.173 MeV and 1.332 MeV).

The materials were designed for use as HTMs in perovskite solar cells and were for the most part synthesized in-house, partly in a semi-automated manner, while three were obtained commercially.[60–64] The material library was put together in

three steps, following the initial assumption that ultraviolet-C (UVC) stability might correlate with gamma stability, which, however, was not confirmed by our results (Fig. S11). Firstly, 24 materials distributed along the UVC stability ranking of our previous study were degraded.[65] Secondly, 21 additional materials of similar structure as the stable materials of the first experiment were tested. Lastly, the most UVC stable material was degraded with gamma radiation.[65] The resulting material library – separated into their core and side units – is shown in Fig. 1a, highlighting the variety in bonds, heteroatoms and functional units. The complete chemical structures of the molecules can be found in Fig. S1. Inert gamma degradation studies on thin films of these materials were then conducted according to the following workflow (Fig. 1b, SI): firstly, chloroform solutions of the materials were spin-coated (static, 600 rpm) onto glass substrates, facilitating device-like layers. To investigate the degradation inside a large Co-60 source at inert conditions, the samples were then encapsulated with another glass substrate using a frame gasket inside a glovebox. The encapsulation was successfully checked for hermetic sealing performance (Fig. S2). The reason for choosing glass substrates is that they do not disintegrate under gamma radiation, keeping the layer inside isolated from any extrinsic effects even at high doses. Two films of each material were then degraded under gamma radiation by placing them inside a so-called phantom in front of the Co-60 source (Fig. S3). Because of the latter, the gamma photons need to pass through 1 cm of polymethyl methacrylate (PMMA), ensuring uniform irradiation of the organic film by fast electrons (green arrows) and cascades of secondary electrons, which dominate the TID damage. The homogeneous ionizing dose is accurately monitored throughout the experiment, and the samples are removed for *ex situ* UV-vis measurements at different stages during the gamma dose accumulation. As can be seen in Fig. 1b, the samples show substantial darkening due to color center formation in the glass substrates during degradation. The corresponding bands are removed from the UV-vis spectra of the samples by subtracting the spectra of the reference stacks (no organic layer), which are degraded at the same time as the samples (Fig. S4 and S5). This way, the characteristic peaks of the organic films can be successfully recovered. As the color center formation is dependent on the glass batch (Fig. S6), attention needs to be paid to using glass substrates from the same batch for both the sample and reference stack. The complete UV-vis dataset after reference correction is provided in SI File A. Furthermore, the UV-vis spectra revealed a jumping baseline – not adhering to a trend – in many cases, which was corrected by performing a linear fit to the tail and subtracting it from the whole spectrum (Fig. S7 and S8). After performing these spectral corrections (Fig. S9), stability targets could be extracted from the UV-vis evolutions to rank the materials by stability and to make a predictive model based on ~1900 structural and semi-empirical computational chemistry descriptors generated from the materials' Simplified Molecular Input Line Entry System (SMILES) codes. Fig. 1c shows the UV-vis evolution of the organic layer of one of the materials after color center and baseline correction, revealing a continuous peak absorbance decrease which could not be observed in the uncorrected spectra (Fig. S5).
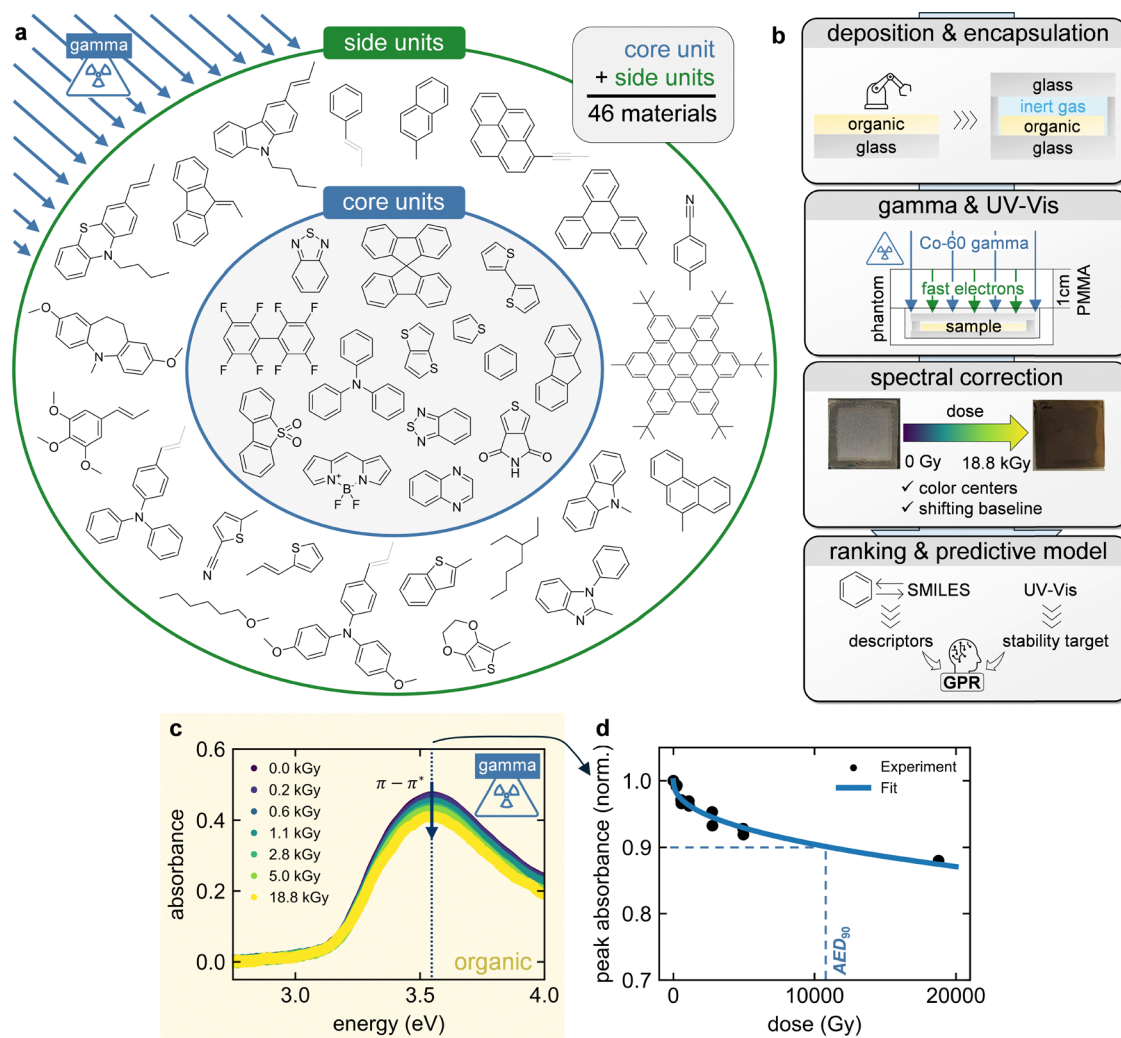
This journal is © The Royal Society of Chemistry 2026

Energy Environ. Sci., 2026, **19**, 635–647 | **637**

Fig. 1 Materials, experimental workflow and data processing of degradation experiments. (a) Library of 46 molecular semiconductors undergoing gamma degradation, each consisting of a core unit and side units. Grey color indicates that units also appear without the vinylene bond. (b) Outline of the experimental workflow. (c) Corrected UV-vis spectra of the organic film of a sample exposed to an accumulated gamma dose of 18.8 kGy. (d) Evolution of the $\pi-\pi^*$ band absorbance over accumulated gamma dose of (c). By fitting the experimental data, the dose at 90% of the initial absorbance (AED_{90}) can be extracted and used as the stability target of this work.

To compare the materials, the $\pi-\pi^*$ band (dashed black line) is observed, as it is characteristic for the conjugated molecular backbone and thus, its evolution over accumulated gamma dose can quantify the general structural stability of the molecules (Fig. 1d). Furthermore, previous studies have shown that the optical stability of single layers is a useful relative indicator of device stability.[62,66,67] To obtain a scalar stability target, the experimental data – consisting of the data points of both samples of the same material – is fitted and the gamma dose at 90% of the initial peak absorbance is determined. This is the so-called accumulated energy dose at 90% absorbance (AED_{90}), which is similar to the UVC stability target of our previous work.[65] For the fit, a formula trained on organic solar cell degradation data *via* symbolic regression as explained by Song *et al.* was chosen:[68]

$$y(a,b,d) = 1 - \frac{d\left(2d + \sqrt{a+1}\right)^b}{a},$$

where d is the gamma dose in Gray (Gy) and a, b are the fit parameters. This hyperbolic formula can capture both the non-linearity and tailing observed in the dataset.

By determining the stability target AED_{90} of each material (Fig. S10 and Table S1), the organic molecules can be ranked by their gamma stability (Fig. 2a). As can be seen, the stability ranges over more than two orders of magnitude, highlighting that the choice of molecular structure or composition has a significant impact on gamma stability. This ranking is in stark contrast to the UVC stability ranking of our previous work,[65] with gamma-stable materials being UVC unstable and *vice versa*, indicating a difference in degradation mechanisms between the two irradiation sources (Fig. S11). On average, the materials can withstand a total ionizing dose of more than 10 kGy, corresponding to a calculated lifetime of over 2 years in the Van Allen belt at an altitude of around 1000 km in LEO.[38] Note that doses and corresponding lifetimes inferred from gamma tests cannot
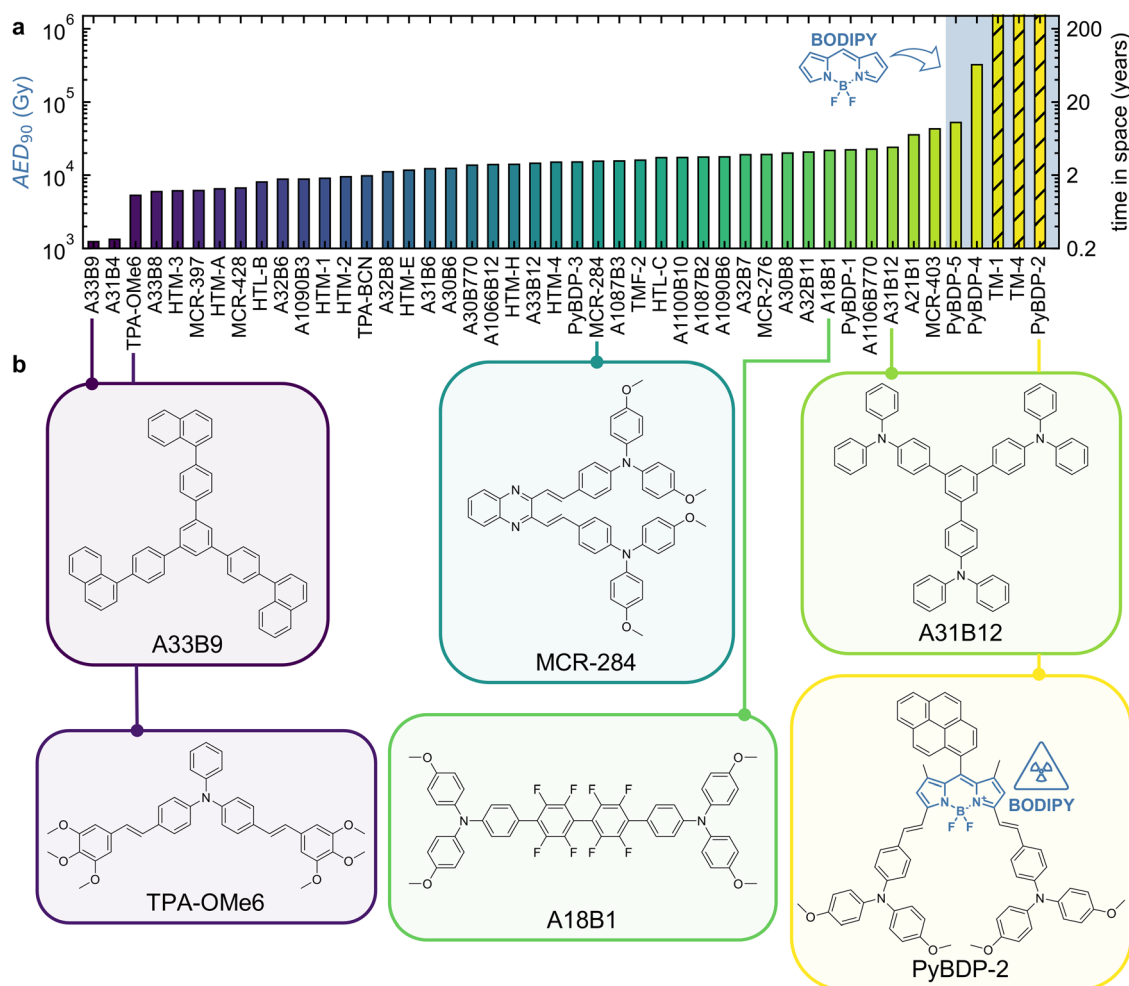
Fig. 2 Gamma stability ranking of molecular semiconductors in inert conditions. (a) Gamma stability ranking of the material library based on the AED_{90} stability target, varying over more than two orders of magnitude, corresponding to calculated lifetimes of 3 months to more than 64 years in the Van Allen belt at an altitude of $\sim$1000 km in LEO. The top 5 most stable materials (blue-shaded background) all feature BODIPY as a center unit, with the top 3 showing a seemingly infinite stability target (diagonal black lines). (b) Representative molecules showing similar structural motifs along the stability ranking.

be directly translated to specific space missions because of the complexity and variability of the space radiation environment and should be regarded as illustrative estimates rather than accurate predictions. Still, such remarkably long lifetimes reveal the high potential of organic materials for use in, *e.g.*, space applications, characterized by an inert environment and persistent ionizing radiation. For comparison, P3HT could also achieve an AED_{90} of more than 10 kGy at vacuum-packaged conditions as investigated by Park *et al.*[46] Furthermore, some materials (TM-1, TM-4, PyBDP-2) do not show any decrease of the π–π* band absorbance within the measured total ionizing dose range (up to 18.8 kGy), and therefore indicate seemingly infinite stability targets, as linear extrapolation to determine a finite AED_{90} is not possible. To still allow for predictive modelling (Fig. 4), the AED_{90} was arbitrarily fixed to 1 000 000 Gy. All materials in the top 5 including the three materials of seemingly infinite stability share BODIPY as the center unit (Fig. S12), drawing special attention to this group for radiation hardness applications. Apart from the BODIPY unit, it is hard to

understand which structural motifs lead to gamma (in)stability. Some representative chemical structures along the stability ranking are shown in Fig. 2b. It is striking that even though molecules look similar, they have vastly different gamma stabilities. A good example is A33B9 *vs.* A31B12, which differ by more than one order of magnitude in stability despite sharing a triphenylbenzene core. The distinguishing structural motif is a peripheral triphenylamine unit. However, this unit appears across the entire stability ranking – alongside other motifs such as methoxy and vinylene groups – underscoring the challenge of finding structure-stability relationships based on the material-dependent ranking. Looking at the atomic composition, it is interesting that all molecules incorporating fluorine atoms (A18B1 and BODIPY molecules) are on the stable side of the stability ranking. This observation is supported by the fact that fluorine has the highest ionization potential out of all heteroatoms used in the present material library, which could explain the high stability of the corresponding molecules against ionizing gamma radiation.

This journal is © The Royal Society of Chemistry 2026

Energy Environ. Sci., 2026, **19**, 635–647 | **639**

A correlation between gamma stability and the highest ionization energy of the molecules' constituent elements can be confirmed by Fig. 3a, although it is relatively weak. Another interesting observation is that there is no correlation between the number of oxygen atoms in a material and the gamma stability AED_{90}. In general, it has been shown that gamma radiation leads to strong oxidation in the presence of oxygen.[22,42,47–49] Even though the samples are not exposed to atmospheric oxygen in this work, it has been suggested that oxygen atoms within the molecular structure may also accelerate degradation if active oxygen radical species form after radiolysis of the molecule.[50] Such an effect cannot be observed in the present material library, as no correlation between the number of oxygen atoms within a molecule and the gamma stability target can be found (Fig. 3b). But even without the interplay of oxygen, bonds and therefore conjugation can break if the energy of the radiation is large enough. However, no correlation between gamma stability and the number of vinylene bonds – a group vulnerable to chain scission and important for predicting UVC stability in our previous work – can be found (Fig. 3c).[65,69,70] A reason why molecules with vulnerable molecular units can seem to be stable is that these materials may interact with fewer photons relative to the rest. In Fig. 3d, the relationship between the AED_{90}

and the absorbed fraction of gamma photons $\gamma_{Ph} = 1 - e^{-\left(\frac{\mu}{\rho}\right) \times \rho \times d}$ is shown. For the latter, the compound's weighted elemental mass

attenuation coefficients $\frac{\mu}{\rho}$ at 1.25 MeV were taken from the NIST XCOM database, and a thickness d of 100 nm and density ρ of 1.2 g cm^{-3} was assumed for all thin films.[71] As can be seen, all materials interact with a similarly small fraction of incident gamma photons. This is expected, as the studied molecules are of comparable size, contain similar atoms of low atomic numbers and were processed at the same conditions. Therefore, it cannot be argued that some layers are just stable because they absorb significantly fewer gamma photons. Instead, the low fractions of absorbed gamma photons highlight that TID damage is dominated by secondary electrons.

To better understand the structure–stability relationships that might impact ionizing radiation tolerance of molecular semiconductors beyond the few preconceived considerations of Fig. 3, we applied predictive modelling to a broad descriptor set, as the limited prior knowledge on design rules for gamma-stable organic materials calls for an open exploration of possible correlations. Another reason is that single-dimensional correlations, as done in Fig. 3, are inherently limited when molecules differ in more than one structural feature, as demonstrated for the case of vinylene bonds in Fig. S13. Even though materials without vinylene are on average more stable than materials with vinylene, they also always differ in at least one other feature and thus, the instability cannot be clearly assigned to vinylene groups. This calls for an approach that tests multi-dimensional
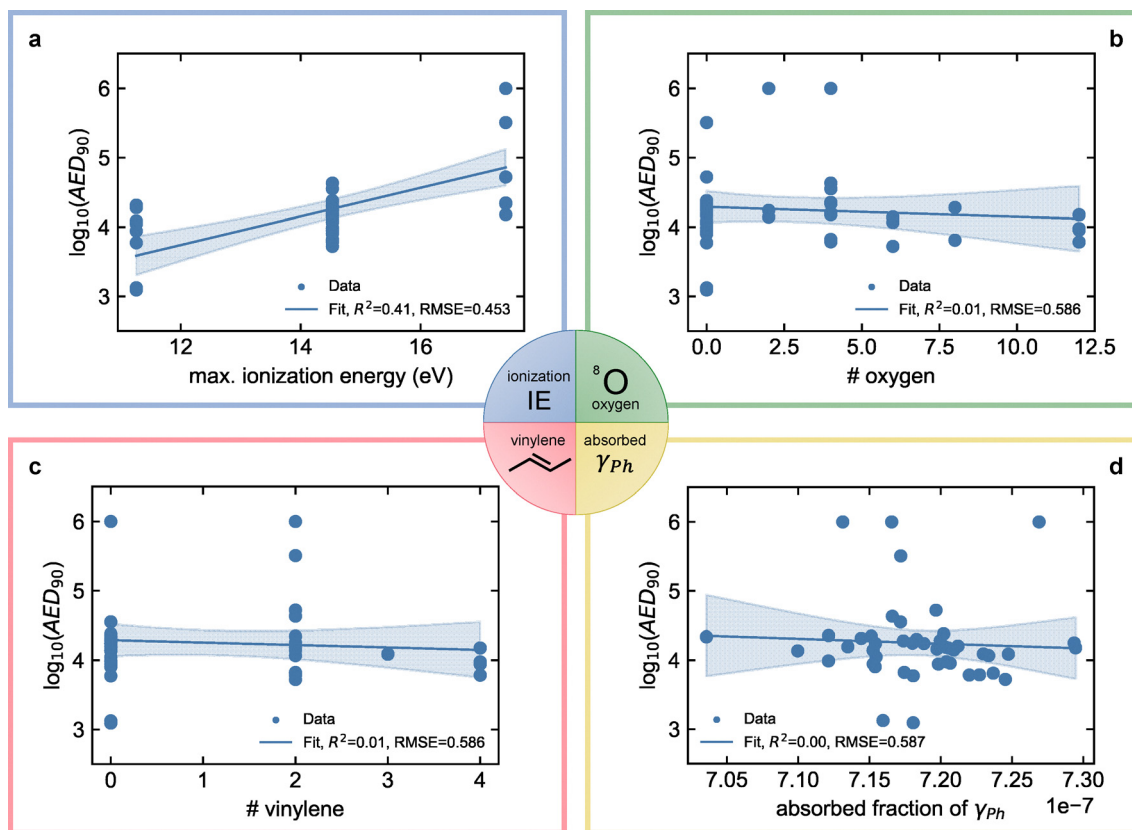

Fig. 3 Relationships between the gamma stability target AED_{90} and sample properties: (a) maximum ionization energy, (b) number of oxygen atoms, (c) number of vinylene bonds, and (d) absorbed fraction of gamma photons γ_{Ph}. The data points are fitted by linear regression (blue line) at a 95% confidence interval (blue-shaded area).

correlations. For this, more than 1900 structural (Mordred and RDKit)[72,73] and semi-empirical computational chemistry (Qik-Prop module)[74] descriptors were compiled based on the SMILES codes of the 46 materials (Fig. 4a).

These include information on the moieties, constitution, atom & bond properties, energetics (force field, semi-empirical), electronic structure, and polarity for the 46 materials, providing a strong foundation to possibly find reasons for the material-dependent gamma stabilities. The full sheet of descriptors, their definitions and fit qualities can be found in SI File B. After reducing the ~1900 descriptors to the top 30, a greedy, multi-dimensional, non-linear Gaussian process regression (GPR) procedure was started to find the best set of predictors for the $\log_{10}(AED_{90})$ gamma stability target. Details on the minimum redundancy maximum relevance (mRMR) feature selection workflow and the greedy additive GPR are provided in the SI and previous works.[65,75,76] The resulting predictive model is shown in Fig. 4b. Strikingly, the model is not able to reproduce the experimental variety in gamma stabilities, and instead splits the dataset into two distinct stability clusters. The reason is that the number of boron atoms was chosen as the sole predictor by the model, yielding a high stability when boron is present and a lower one when it is not (Fig. 4c). In other words, BODIPY molecules are stable (1 boron atom), while the rest is not. As a disclaimer, an identical model with the number of BODIPY units instead of the number of boron atoms can be produced, as both descriptors have the exact same values for the individual materials. Although this attempt at a predictive model might seem like a failure, as the result is immediately deducible from the stability ranking, it has big implications: out of more than 1900 important material properties (Fig. 4a), none outperforms the number of boron atoms in terms of relevance and independence. The seemingly linear model even prevails over multi-descriptor models that are not constrained in non-linearity. On the one hand, this provides the insight that no significant correlation exists for all these parameters, narrowing down future investigations. On the other hand, it highlights the importance of understanding the unknown reason for the stabilizing effect of the boron atom or the BODIPY unit it is embedded in. While boron is integral to boron carbides known for their neutron-shielding capabilities, their radiation hardness does not stem from boron *per se* but from the 3D network of σ-aromatic icosahedra - formed by three-center-two-electron (3c-2e) σ-bonding borons – capable of accommodating displacement damage.[77–80] By contrast, BODIPY contains a single four coordinate boron center with conventional 2c-2e boron bonds embedded in a π-conjugated 2D framework. Therefore, the lattice-level defect-tolerant mechanisms of boron carbides do not transfer to BODIPY. One distinct property that distinguishes the BODIPY molecules from the rest is their comparatively low optical band gap of around 1.75 eV, placing them *ca.* 1.5 eV below the other materials in the library (Fig. S14). This represents a substantial difference of about 1.5 eV, which could influence how dense cascades of secondary electrons with energies down to a few eV interact with the material. Therefore, apart from testing non-BODIPY boron-containing molecules to assign stability to either the boron atom
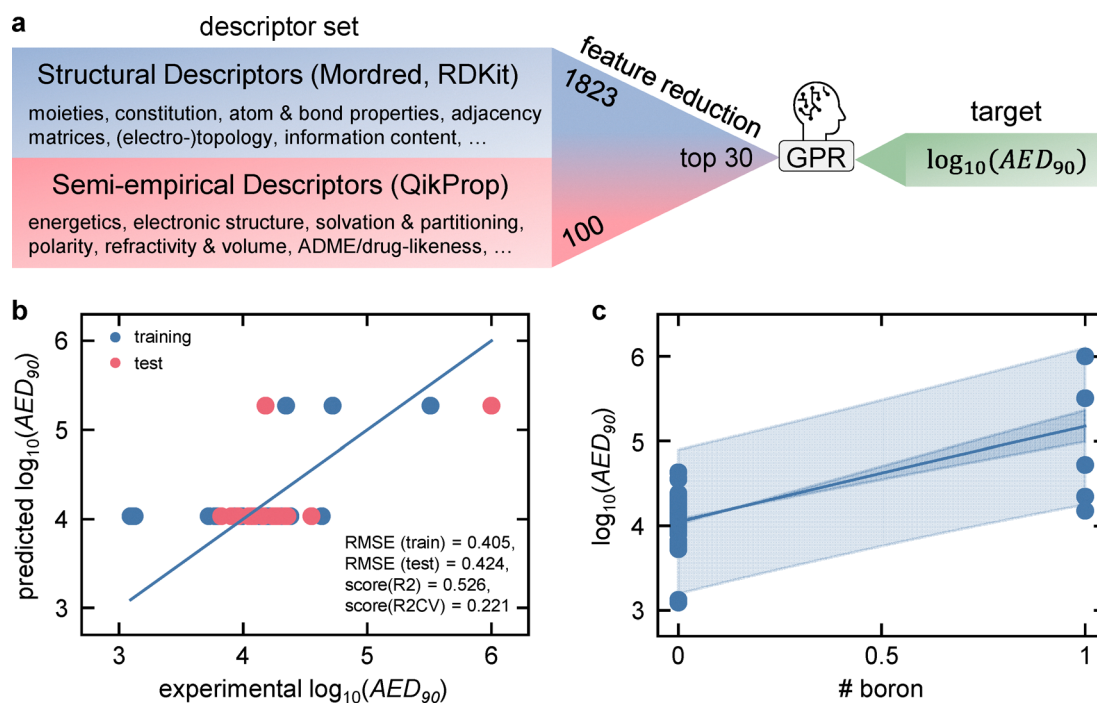

Fig. 4 Predictive model for gamma radiation stability. (a) Overview of the predictive modelling workflow consisting of a descriptor set of more than 1900 structural and semi-empirical computational chemistry features, and its reduction to the top 30 least redundant and most relevant features, followed by GPR with respect to the $\log_{10}(AED_{90})$ gamma stability target. (b) Predictive model for gamma stability ($\log_{10}(AED_{90})$) resulting from the workflow described in (a). (c) Dependence of the gamma stability ($\log_{10}(AED_{90})$) on the number of boron atoms as the sole predictor of the model in (b).

This journal is © The Royal Society of Chemistry 2026

Energy Environ. Sci., 2026, **19**, 635–647 | **641**

or BODIPY itself and employing quantum-chemical calculations to elucidate the underlying physics of BODIPY's gamma stability, testing more materials with low optical band gaps is advisable.

To explore possible degradation mechanisms caused by gamma-ray exposure, the evolutions of the UV-vis spectra are studied in more detail, analyzing the whole spectral range.

In Fig. 5a, increasing absorbance in the tail region of the spectra (low energies) is studied, which could possibly point towards the formation of transient states. The differential absorbance spectra of material A1090B3 (Fig. 5a, upper panel) resemble characteristic dynamics in transient absorption spectra evident for charge generation: ground state bleach (GSB, left blue arrow) and excited state absorption (ESA, right blue arrow). The oscillatory signature of the GSB (minimum) and ESA (maximum) peaks could also be interpreted as a sign of electro-absorption (Stark effect).[81] The latter is unlikely in the present sample, as fitting the differential absorption spectrum (4500 Gy – 0 Gy) with a combination of the 0 Gy absorbance spectrum $A(E)$ and its first and second derivatives ($A'(E)$, $A''(E)$) reveals that $A(E)$ has the highest contribution, while the contribution of $A''(E)$ is negligible (Fig. S15).[82] This points towards an absorbance-like intensity change and not to a derivative-type Stark signal. Furthermore, charge generation is probably not the reason for the strong increase at longer wavelengths, as the absorbance change is still present after storing the sample in an inert atmosphere for 10 months. UV-vis changes due to transient charge carriers should have recovered by then. Therefore, permanent changes to the

layer, such as scattering and polymerization could be reasonable explanations.[55,83] In contrast, material A32B7 (Fig. 5a, lower panel) shows strong recovery of the tail region after 10 months, dropping back down to the level of around 200 Gy. In this case, transient states like polaron formation are a likely mechanism. Another possibility is the formation of a singly occupied molecular orbital (SOMO) following the trapping of an electron in an oxygen vacancy of the glass.[84–87] Depending on the depth, these states can either be short or long-lived.[88] Looking at all materials showing a clear absorbance increase at low energies (Fig. S16), it becomes evident that the degree of recovery is mixed: while most of them show recovery in the tail region to a varying degree, some retain their absorbance change even after 10 months. This means that, on the one hand, changes to the materials during gamma-ray exposure are not necessarily permanent, and on the other hand, formation of states with material-dependent lifetimes could be possible. Interestingly, many materials also show a recovery of the main absorption band (Fig. S17) and of regions at even higher energies (Fig. S18). Only 2 (MCR-428, PyBDP-1) out of the 16 re-measured materials show no clear recovery of the π–π* band, suggesting that recovery may be a general phenomenon for organic semiconductors under the conditions of this work (Fig. S19). An absorbance decrease in these regions is typically associated with structural degradation of the conjugated system (chromophore) or more localized molecular groups (high energy). Fig. 5b shows that, as evident from, e.g., TM-4 (upper panel), absorbance decreases at higher energies beyond the π–π* band,
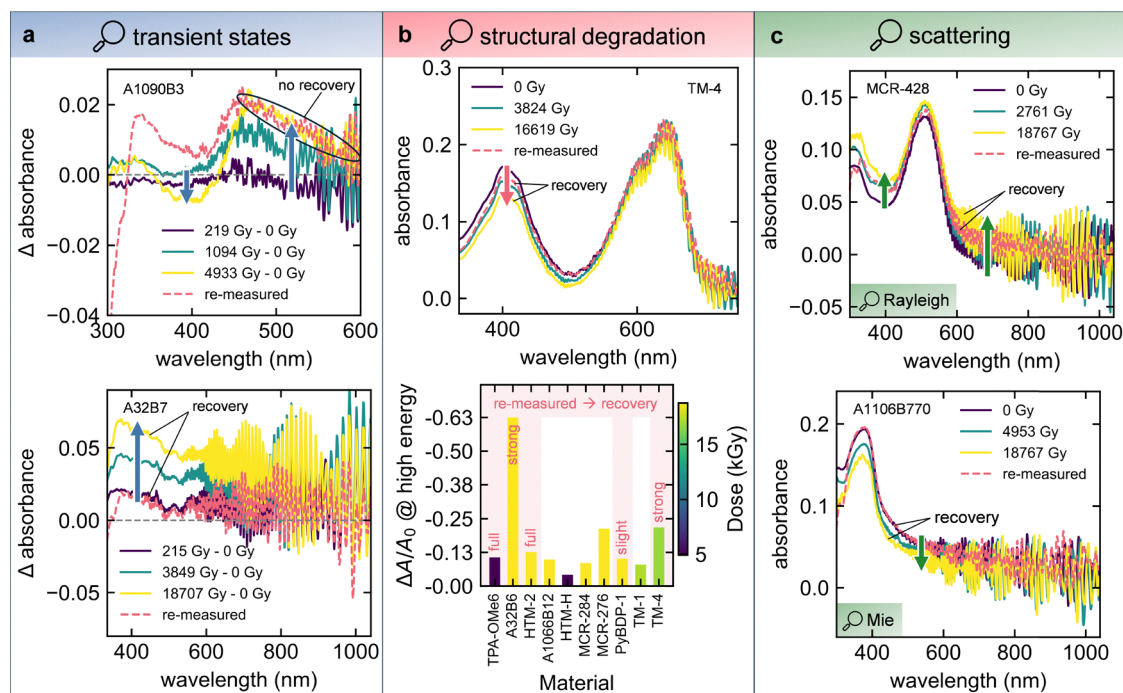

Fig. 5 Mechanistic exploration *via* analysis of UV-vis evolutions. (a) Study of transient states probed through the absorbance increase at low energies during degradation for A1090B3 (upper panel) and A32B7 (lower panel). (b) Exploration of structural degradation probed through the absorbance decrease at high energies for the example of TM-4 (upper panel). Summary of the normalized differential signal at high energies for a selection of materials. The red background highlights materials showing a varying degree of UV-vis recovery at high energies. The rest has not been re-measured. (c) Investigation of scattering through the absorbance change at low and high energies by the examples of MCR-428 (Rayleigh scattering) and A1106B770 (Mie scattering). The dashed red curves refer to re-measurements of the samples 10 months after gamma degradation.

642 | *Energy Environ. Sci.*, 2026, **19**, 635–647

This journal is © The Royal Society of Chemistry 2026

which is not captured by the AED_{90} stability target. Therefore, even materials with a stable chromophore are potentially subjected to structural degradation of their more localized groups. However, the 400 nm peak recovers after 10 months of storage time, suggesting reversibility of the structural degradation. In the lower panel of Fig. 5b, all materials showing a clear decrease at high energies are summarized (Fig. S20). It has to be mentioned that analyzing changes beyond the $\pi-\pi^*$ band is not possible for all materials due to this region being outside the measurement/transparency range. Generally, an absorbance decrease at high energies seems to correlate with an increasing gamma-ray dose (see color bar). However, it does not correlate with the AED_{90} target (materials are sorted from left to right in ascending AED_{90} order), meaning that stable materials are potentially subjected to significant structural degradation of localized groups and vice versa. From the materials that have been re-measured a long time after the degradation experiments (TPA-OMe6, A32B6, HTM-2, PyBDP-1, TM-4), all of them show up to strong or even full recovery of the complete UV-vis spectrum, including the $\pi-\pi^*$ band (Fig. S17) and – in the cases where it could be resolved in the re-measurement – the high-energy region (Fig. S18). This implies that adverse changes induced by gamma radiation may be reversible, returning the materials to their pristine state, which means that the AED_{90} stability target does not necessarily capture only irreversible structural changes (e.g. bond-breaking).[89,90] As this could increase the lifetime of organic semiconductors and devices subjected to radiation-hard environments, further studies to understand the mechanism and potentially accelerate it are crucial. A possibility is isomerization of the molecules, which reverses in a radiation-free environment.[91–93] Lastly, some materials seem to start exhibiting scattering as a result of degradation, while others display modifications to pre-existing scattering signatures. MCR-428 (Fig. 5c, upper panel), MCR-397 and HTM-E (Fig. S21) – not bearing signs of scattering before degradation – start to show a broad absorbance increase across the UV-Vis spectrum after degradation. The pronounced rise at higher energies could be related to Rayleigh scattering, which follows a $\sim \lambda^{-4}$ dependence. However, after re-measuring MCR-428 10 months after degradation, much of the absorbance increase has recovered, especially in the high-energy region. Therefore, the scattering centers formed during degradation either recovered, or scattering was never present. Instead, changes at low energies could point towards mechanisms discussed in Fig. 5a, and changes at high energies could be related to radiation-induced isomerization or radical formation.[94,95] A1106B770 (Fig. 5c, lower panel) and A32B11 (Fig. S22) show a slowly decaying baseline before degradation, which is characteristic of Mie scattering. During degradation, the baseline decreases, potentially meaning that scattering centers shrink in size. However, after re-measuring A1106B770 10 months after the degradation, the UV-vis spectrum has fully recovered. Similar to the situation in the upper panel of Fig. 5c, the scattering centers either transformed back to their original state/size or the slowly decaying baseline is not related to scattering but is, e.g., an Urbach tail, reflecting sub-bandgap absorption. Future work could clarify whether the examples in Fig. 5c originate from changes in scattering behavior by

employing haze measurements and specular vs. total transmission experiments with an integrating sphere before, during, and after degradation. Overall, the secondary effects presented in Fig. 5, which include both changes and recovery in the UV-Vis spectrum, suggest that the employed AED_{90} stability target, and consequently the ranking, reflects not only irreversible structural changes but also other gamma-induced degradation and recovery phenomena. This underscores the complexity of gamma degradation studies and highlights the importance of carefully defining the stability target. In order to study the possible proposed mechanisms behind the observed recovery – namely polaron formation, trapping in oxygen vacancies, isomerization and scattering – performance of UV-vis measurements of the re-dissolved film, ESR of the glass substrates, NMR spectra of the material and transmission measurements with an Ulbricht sphere are suggested, respectively. Furthermore, post-irradiation annealing can be used to generally check whether the recovery can be accelerated by overcoming an activation energy. When comparing the observations made in Fig. 5 with our previous UVC stability study on the same materials, it becomes clear that the degradation mechanisms are entirely different.[65] While UVC degradation was mainly assigned to oxygen- and sulfur-containing units, as well as cleavage of weak bonds, which can be prevented via intramolecular vibrational redistribution facilitated by fused aromatic ring clusters, gamma tests show no signs of this: BODIPY molecules with susceptible vinylene bonds are highly stable and molecules with many fused ring clusters and no heteroatoms are very unstable (Fig. S11). Furthermore, in contrast to the gamma experiments, UVC degradation does not show any recovery of the UV-Vis spectra, indicating that bond cleavage and related processes are permanent (Fig. S23). This observation suggests that irreversible structural changes caused by bond cleavage are not the dominant degradation mechanism during inert gamma irradiation of organic semiconductors. Therefore, even though UVC photons and gamma-induced secondary electron cascades fall into the same energy range, their effects on the material are different, highlighting the importance of testing both in order to arrive at a more universal radiation hardness.

Discussion and conclusions

For the first time, the stability of a large library of molecular semiconductors of varying structures has been systematically studied under gamma radiation at inert conditions, acting as a radiation hardness proxy for the oxygen-free space environment and encapsulated terrestrial applications. The workflow developed in the present study provides a reliable approach to determine the gamma stability of any given organic thin film encapsulated with a glass substrate using UV-vis spectroscopy. As a result, 46 state-of-the-art conjugated molecules designed for use as HTMs in perovskite solar cells could be ranked by their ionizing radiation tolerance, with most materials withstanding a total ionizing dose of over 10 kGy, corresponding to a calculated lifetime of more than 2 years under unshielded radiation in the

This journal is © The Royal Society of Chemistry 2026

Energy Environ. Sci., 2026, 19, 635–647 | 643

Van Allen belt at an altitude of around 1000 km in LEO. Materials incorporating BODIPY even reach up to seemingly infinite gamma radiation tolerance according to the employed optical stability target of this work, showing potential for long-term applications in space. Overall, the stability ranking ranges over more than two orders of magnitude. This indicates that the degradation can be mainly attributed to the secondary electrons, as gamma photons should degrade organics in a comparable manner, since organic materials composed of low-Z elements have similarly small gamma absorption cross-sections and the photon energies involved far exceed typical bond energies. Consequently, there are structure-stability relationships to discover, and, given the already outstanding stabilities of a material library selected without prior knowledge of gamma-stability design rules, more efforts hold promise to leverage the many advantages of organic semiconductors in solar cells, sensors and transistors for use in harsh radiation environments. While studying preconceived considerations based on the limited knowledge on radiation hardness of molecular semiconductors could confirm that all materials of the present library interact with very similar small amounts of gamma photons and that elements with a high ionization potential likely have a positive effect on the ionizing radiation tolerance, they are not able to explain the strong variation of the gamma stability ranking, calling for a broader and open investigation. Therefore, multi-dimensional non-linear predictive modelling on more than 1900 structural and semi-empirical computational chemistry descriptors was performed. Interestingly, the established model is only based on one single predictor, namely the number of boron atoms. It therefore conveys that BODIPY molecules (1 boron atom) are significantly more stable than all other molecules of the present material library (0 boron atoms). Although this is easily deducible from the stability ranking which is led by BODIPY molecules, it makes the important implication that there is no correlation between the stability target and the other 1900 descriptors that could outperform the number of boron atoms in relevance and independence. This helps to narrow down future studies to parameters that have not been investigated in this work and also assures a lot of freedom in the material design of ionizing radiation tolerant materials for tailored applications. Furthermore, it emphasizes the importance of understanding the stabilizing properties of the boron atom or the BODIPY moiety it is embedded in. Promising future directions include experimental studies on both BODIPY and non-BODIPY boron-containing molecules to clarify whether the stability originates from the boron atom or the BODIPY framework, as well as quantum-chemical calculations to refine the predictive model built on the present dataset. Additionally, the high stabilities of the BODIPY molecules at comparatively low band gaps motivate studies on more low band gap materials, such as polymer donors and non-fullerene acceptors used in the active layer of organic solar cells. Ongoing studies already indicate promising results. Analyzing the evolutions of the UV-vis spectra throughout gamma degradation further highlights the complexity of the interaction between gamma radiation and molecular semiconductors. Apart from decreasing absorbance in the π–π^* band normally assigned to photobleaching and tracked by the employed stability target of this work, there is also material-dependent increase or decrease of absorbance at the low and high energy regions of the UV-vis spectra. These can possibly be assigned to other mechanisms than the anticipated decomposition of the molecules and might interfere in the evolution of the π–π^* band, thus complicating developing a general predictive model for gamma-stable organic semiconductors. Many of the studied materials either show an increase at low energies in the tail region of the spectra or a decrease at high energies beyond the π–π^* band, which could be linked to the formation of transient states or isomerization of certain molecules, respectively. In both cases, up to full recovery of the UV-vis spectra was observed for many of the materials 10 months after degradation. Furthermore, some samples appear to show changes in their scattering behavior during gamma exposure followed by recovery. To elucidate the origin of the reversible behavior, we suggest UV-Vis measurements of re-dissolved films, ESR of the glass substrates, NMR spectra of the materials, and transmission measurements using an Ulbricht sphere. In addition, post-irradiation annealing experiments could be used to assess whether the recovery can be accelerated by overcoming an activation energy.

In conclusion, this work demonstrates the remarkable ionizing radiation tolerance of organic semiconductors. The outstanding stability of BODIPY provides strong motivation for the development of new materials based on this unit and studies on the incorporation of multiple BODIPY moieties, extended architectures such as BOIMPY (bis(borondifluoride)-8-imidazodipyrromethene) and inclusion of other boron complexes such as triarylboranes and subphthalocyanines. In addition to high stability, the observed recovery of the UV-vis spectra during radiation-free intervals suggests that material lifetimes may reset, which in turn calls for device-level investigation. The methodology presented in this work – an inert gamma irradiation protocol for (organic) thin films – offers a reliable framework for such studies and for further investigating the degradation mechanisms and underlying physics. Looking ahead, quantum-chemical calculations, together with an expanded dataset aiming at increasing atomistic and structural diversity, could enable predictive models for the inverse design of gamma-stable molecular semiconductors for space and specialized terrestrial applications.

Author contributions

A. J. B., A. J. M., L. L., and C. J. B. designed the study. A. J. B. and A. J. M fabricated the samples. A. J. M. and J. A. P. performed the gamma degradation and UV-vis characterization experiments under the supervision of J. B. D. at the radiation facility (ANSTO). A. J. B. evaluated the experimental data with support from A. J. M. J. W., J. S. R. O., and M. C. R. provided the materials for this work. P. D. calculated the semi-empirical computational chemistry descriptors. L. L. set up the machine learning and feature selection workflow. A. J. B. wrote the original draft of the manuscript. A. J. M., L. L., and C. J. B revised the manuscript. A. J. M., A. O., B. I., D. Z., M. P., L. L.,

644 | *Energy Environ. Sci.*, 2026, **19**, 635–647

This journal is © The Royal Society of Chemistry 2026

and C. J. B. supervised the project. All authors reviewed and accepted the manuscript.

Conflicts of interest

The authors declare no conflict of interest.

Data availability

The data supporting this article have been included as part of the supplementary information (SI). SI File A contains the complete UV-vis dataset after reference correction. SI File B provides the full sheet of descriptors, their definitions and fit qualities. See DOI: https://doi.org/10.1039/d5ee05453b.

Acknowledgements

References

1 M. Höyhtyä, *Satellite Communications and Networks*, Springer Nature, Switzerland, Cham, 2025.

2 A. R. Kirmani and I. R. Sellers, *Joule*, 2025, **9**, 101852.

3 W. L. Megginson, *Social Science Research Network*, 2024, preprint, 4901992, DOI: 10.2139/ssrn.4901992.

4 H. Zhu, M. L. K. Chua, I. Chitapanarux, O. Kaidar-Person, C. Mwaba, M. Alghamdi, A. R. Mignola, N. Amrogowicz, G. Yazici, Z. Bourhaleb, H. Mahmood, G. M. Faruque, M. Thiagarajan, A. Acharki, M. Ma, M. Harutyunyan, H. Sriplung, Y. Chen, R. Camacho, Z. Zhang and M. Abdel-Wahab, *Lancet Glob. Health*, 2024, **12**, e1945–e1953.

5 K. Ding and C. Makanjee, *BMC Geriatr.*, 2024, **24**, 205.

6 M. D. Mathew, *Prog. Nucl. Energy*, 2022, **143**, 104080.

7 J. A. Posar, M. Petasecca and M. J. Griffith, *Flex. Print. Electron.*, 2021, **6**, 043005.

8 M. J. Griffith, S. Cottam, J. Stamenkovic, J. A. Posar and M. Petasecca, *Front. Phys.*, 2020, **8**, 22.

9 M. Chen, C. Wang and W. Hu, *J. Mater. Chem. C*, 2021, **9**, 4709–4729.

10 A. Panagiotopoulos, T. Maksudov, G. Kakavelakis, G. Perrakis, E. A. Alharbi, D. Kutsarov, F. H. Isikgor, S. Alfihed, K. Petridis, M. Kafesaki, S. R. P. Silva, T. D. Anthopoulos and M. Graetzel, *Appl. Phys. Rev.*, 2023, **10**, 041303.

11 S. Xiong, K. Fukuda, S. Lee, K. Nakano, X. Dong, T. Yokota, K. Tajima, Y. Zhou and T. Someya, *Adv. Sci.*, 2022, **9**, 2105288.

12 R. Verduci, V. Romano, G. Brunetti, N. Yaghoobi Nia, A. Di Carlo, G. D'Angelo and C. Ciminelli, *Adv. Energy Mater.*, 2022, **12**, 2200125.

13 S. S. Arnold, R. Nuzzaci and A. Gordon-Ross, in *2012 IEEE Aerospace Conference*, 2012, pp. 1–14.

14 W. Li, C. Zhang, D. Lan, W. Ji and Y. Wang, *Adv. Eng. Mater.*, 2022, **24**, 2200173.

15 L. McMillon-Brown, J. M. Luther and T. J. Peshek, *ACS Energy Lett.*, 2022, **7**, 1040–1042.

16 M. T. Hoang, Y. Yang, B. Tuten and H. Wang, *J. Phys. Chem. Lett.*, 2022, **13**, 2908–2920.

17 Y. Tu, J. Wu, G. Xu, X. Yang, R. Cai, Q. Gong, R. Zhu and W. Huang, *Adv. Mater.*, 2021, **33**, 2006545.

18 M. E. Bush, J. D. Sims, S. S. Erickson, K. T. VanSant, S. Ghosh, J. M. Luther and L. McMillon-Brown, *Acta Astronaut.*, 2025, **235**, 235–250.

19 MIL-STD-883E: Test Method Standard for Microcircuits, U.S. Department of Defense, Washington, D.C., 1989.

20 *MIL-STD-750D: Test Methods for Semiconductor Devices*, U.S. Department of Defense, Washington, D.C., 1987.

21 Q. Chen, T. Hajagos and Q. Pei, *Annu. Rep. Sect. C Phys. Chem.*, 2011, **107**, 298–318.

22 C. Freissinet, M. Millan, D. P. Glavin, X. Li, A. Grubisic, J. E. Eigenbrode, J. C. Stern, J. P. Dworkin, A. Buch, C. Szopa, M. A. Guzman, M. A. Carts, S. A. Getty and W. B. Brinckerhoff, *Planet. Space Sci.*, 2019, **175**, 1–12.

23 G. P. Summers, E. A. Burke, P. Shapiro, S. R. Messenger and R. J. Walters, *IEEE Trans. Nucl. Sci.*, 1993, **40**, 1372–1379.

24 J. P. Raymond and E. L. Petersen, *IEEE Trans. Nucl. Sci.*, 1987, **34**, 1621–1628.

25 R. W. Tallon, M. R. Ackermann, W. T. Kemp, M. H. Owen and D. P. Saunders, *IEEE Trans. Nucl. Sci.*, 1985, **32**, 4393–4398.

26 G. J. Brucker, E. G. Stassinopoulos, O. Van Gunten, L. S. August and T. M. Jordan, *IEEE Trans. Nucl. Sci.*, 1982, **29**, 1966–1969.

27 V. N. Hegde, T. M. Pradeep, N. Pushpa, K. C. Praveen, K. G. Bhushan, J. D. Cressler and A. P. Gnana Prakash, *IEEE Trans. Device Mater. Reliab.*, 2018, **18**, 592–598.

28 G. Akhtanova, H. P. Parkhomenko, N. Asanov, A. I. Mostovyi, N. Schopp, M. Kaikanov and V. V. Brus, *Adv. Opt. Mater.*, 2025, **13**, 2501396.

29 Y. Li, K. Kamaraj, Y. Silori, H. Zhao, C. Arneson, B. Liu, J. Ogilvie and S. R. Forrest, *Joule*, 2025, **9**, 101800.

30 H. P. Parkhomenko, M. M. Solovan, S. Sahare, A. I. Mostovyi, D. Aidarkhanov, N. Schopp, T. Kovaliuk, M. Kaikanov, A. Ng and V. V. Brus, *Adv. Funct. Mater.*, 2024, **34**, 2310404.

31 S. Erickson, C. Lum, K. Stephens, M. Parashar, D. K. Saini, B. Rout, C. Park, T. J. Peshek, L. McMillon-Brown and S. Ghosh, *iScience*, 2025, **28**, 111586.

This journal is © The Royal Society of Chemistry 2026

Energy Environ. Sci., 2026, **19**, 635–647 | **645**

32 H. Shim, S. Seo, C. Chandler, M. K. Sharpe, C. D. McAleese, J. Lim, B.-S. Kim, S. Roy, I. Jayawardena, S. R. P. Silva, M. A. Baker, J. Seidel, M. A. Green, H. J. Snaith, D. Kim, J. Park and J. S. Yun, *Joule*, 2025, **9**, 102043.

33 Z. Cai, Y. Wu and S. Chen, *Appl. Phys. Lett.*, 2021, **119**, 123901.

34 A. R. Kirmani, B. K. Durant, J. Grandidier, N. M. Haegel, M. D. Kelzenberg, Y. M. Lao, M. D. McGehee, L. McMillon-Brown, D. P. Ostrowski, T. J. Peshek, B. Rout, I. R. Sellers, M. Steger, D. Walker, D. M. Wilt, K. T. VanSant and J. M. Luther, *Joule*, 2022, **6**, 1015–1031.

35 Z. Huan, Y. Zheng, K. Wang, Z. Shen, W. Ni, J. Zu and Y. Shao, *J. Mater. Chem. A*, 2024, **12**, 1910–1922.

36 L. Zhang, S. Li, Y. Wang, H. Li, R. Chen, X. Zhu, X. Xu, Y. Hao and Y. Ma, *Mater. Adv.*, 2025, **6**, 8490–8496.

37 Integrated Circuits (Microcircuits) Manufacturing, General Specification for, U.S. Department of Defense, Washington, D.C., 2002.

38 A Guide to Space Radiation, Bureau of Meteorology, Space Weather Services, Commonwealth of Australia, 2016.

39 A. Ciavatti, L. Basiricò, I. Fratelli, S. Lai, P. Cosseddu, A. Bonfiglio, J. E. Anthony and B. Fraboni, *Adv. Funct. Mater.*, 2019, **29**, 1806119.

40 S. Baccaro, P. D'Atanasio, S. Talice, M. Gennis, G. Marini, M. Mattioli and A. Nigro, *Int. J. Radiat. Appl. Instrum.*, 1992, **40**, 585–587.

41 M. Wolszczak, J. Kroh and M. M. Abdel-Hamid, *Radiat. Phys. Chem.*, 1995, **45**, 71–78.

42 H. N. Raval, D. S. Sutar, P. R. Nair and V. Ramgopal Rao, *Org. Electron.*, 2013, **14**, 1467–1476.

43 E. A. B. Silva, J. F. Borin, P. Nicolucci, C. F. O. Graeff, T. G. Netto and R. F. Bianchi, *Appl. Phys. Lett.*, 2005, **86**, 131902.

44 A. Kumar Anbalagan, S. Gupta, M. Chaudhary, R. Ranjan Kumar, Y.-L. Chueh, N.-H. Tai and C.-H. Lee, *RSC Adv.*, 2021, **11**, 20752–20759.

45 A. Todd, T. Zhu, F. Zhang, C. Zhang, A. Berger and J. Xu, *ECS Trans.*, 2009, **25**, 103.

46 C. H. Park, J. Park and F. S. Kim, *Mol. Cryst. Liq. Cryst.*, 2019, **687**, 1–6.

47 S. Park, S. Choi, H. Lee, J. Lee, Y. Woo, Y.-J. Jung, Y. M. Jung, J. Jeong, J. Park, Y. Yi, S. Park and H. Lee, *Polym. Degrad. Stab.*, 2021, **186**, 109518.

48 H. N. Raval, S. P. Tiwari, R. R. Navan and V. R. Rao, *Appl. Phys. Lett.*, 2009, **94**, 123304.

49 J. M. G. Laranjeira, H. J. Khoury, W. M. de Azevedo, E. A. de Vasconcelos and E. F. da Silva, *Mater. Charact.*, 2003, **50**, 127–130.

50 H. H. Tokhy, E. K. Elmaghraby, A. M. Abdelhady, A. M. Eid, Y. S. Rammah, E.-S. M. Awad and S. Abdelaal, *Radiochim. Acta*, 2021, **109**, 407–418.

51 Y. Xu, J. Bi, K. Xi and M. Liu, *Appl. Phys. Express*, 2019, **12**, 061004.

52 N. Sai, K. Leung, J. Zádor and G. Henkelman, *Phys. Chem. Chem. Phys.*, 2014, **16**, 8092–8099.

53 J. Guo, Y. Wu, R. Sun, W. Wang, J. Guo, Q. Wu, X. Tang, C. Sun, Z. Luo, K. Chang, Z. Zhang, J. Yuan, T. Li, W. Tang, E. Zhou, Z. Xiao, L. Ding, Y. Zou, X. Zhan, C. Yang, Z. Li, C. J. Brabec, Y. Li and J. Min, *J. Mater. Chem. A*, 2019, **7**, 25088–25101.

54 M. K. Choudhary and S. Mula, *New J. Chem.*, 2023, **47**, 9045–9049.

55 A. Ashfaq, M.-C. Clochard, X. Coqueret, C. Dispenza, M. S. Driscoll, P. Ulański and M. Al-Sheikhly, *Polymers*, 2020, **12**, 2877.

56 E. S. Wirström, S. B. Charnley, M. A. Cordiner and C. Ceccarelli, *Astrophys. J.*, 2016, **830**, 102.

57 A. Luspay-Kuti, O. Mousis, J. I. Lunine, Y. Ellinger, F. Pauzat, U. Raut, A. Bouquet, K. E. Mandt, R. Maggiolo, T. Ronnet, B. Brugger, O. Ozgurel and S. A. Fuselier, *Space Sci. Rev.*, 2018, **214**, 115.

58 B. Larsson, R. Liseau, L. Pagani, P. Bergman, P. Bernath, N. Biver, J. H. Black, R. S. Booth, V. Buat, J. Crovisier, C. L. Curry, M. Dahlgren, P. J. Encrenaz, E. Falgarone, P. A. Feldman, M. Fich, H. G. Florén, M. Fredrixon, U. Frisk, G. F. Gahm, M. Gerin, M. Hagström, J. Harju, T. Hasegawa, Å. Hjalmarson, L. E. B. Johansson, K. Justtanont, A. Klotz, E. Kyrölä, S. Kwok, A. Lecacheux, T. Liljeström, E. J. Llewellyn, S. Lundin, G. Mégie, G. F. Mitchell, D. Murtagh, L. H. Nordh, L.-Å. Nyman, M. Olberg, A. O. H. Olofsson, G. Olofsson, H. Olofsson, G. Persson, R. Plume, H. Rickman, I. Ristorcelli, G. Rydbeck, A. A. Sandqvist, F. V. Schéele, G. Serra, S. Torchinsky, N. F. Tothill, K. Volk, T. Wiklind, C. D. Wilson, A. Winnberg and G. Witt, *Astron. Astrophys.*, 2007, **466**, 999–1003.

59 I. V. Martynov, A. V. Akkuratov, S. Y. Luchkin, S. A. Tsarev, S. D. Babenko, V. G. Petrov, K. J. Stevenson and P. A. Troshin, *ACS Appl. Mater. Interfaces*, 2019, **11**, 21741–21748.

60 J. Wu, J. Zhang, M. Hu, P. Reiser, L. Torresi, P. Friederich, L. Lahn, O. Kasian, D. M. Guldi, M. E. Pérez-Ojeda, A. Barabash, J. S. Rocha-Ortiz, Y. Zhao, Z. Xie, J. Luo, Y. Wang, S. I. Seok, J. A. Hauch and C. J. Brabec, *J. Am. Chem. Soc.*, 2023, **145**, 16517–16525.

61 J. Wu, L. Torresi, M. Hu, P. Reiser, J. Zhang, J. S. Rocha-Ortiz, L. Wang, Z. Xie, K. Zhang, B. Park, A. Barabash, Y. Zhao, J. Luo, Y. Wang, L. Lüer, L.-L. Deng, J. A. Hauch, D. M. Guldi, M. E. Pérez-Ojeda, S. I. Seok, P. Friederich and C. J. Brabec, *Science*, 2024, **386**, 1256–1264.

62 J. S. Rocha-Ortiz, J. Wu, J. Wenzel, A. J. Bornschlegl, J. D. Perea, S. Leon, A. Barabash, A.-S. Wollny, D. M. Guldi, J. Zhang, A. Insuasty, L. Lüer, A. Ortiz, A. Hirsch and C. J. Brabec, *Adv. Funct. Mater.*, 2023, **33**, 2304262.

63 I. Seoneray, J. Wu, J. S. Rocha-Ortiz, A. J. Bornschlegl, A. Barabash, Y. Wang, L. Lüer, J. Hauch, A. García, J. Zapata-Rivera, C. J. Brabec and A. Ortiz, *Sol. RRL*, 2024, **8**, 2400225.

64 M. Caicedo-Reina, J. S. Rocha-Ortiz, J. Wu, A. J. Bornschlegl, S. Leon, A. Barabash, J. Dario Perea, Y. Wang, V. Arango-Marín, A. Ortiz, L. Lüer, J. A. Hauch, B. Insuasty and C. J. Brabec, *Chem. – Eur. J.*, 2025, **31**, e202404251.

65 A. J. Bornschlegl, P. Duchstein, J. Wu, J. S. Rocha-Ortiz, M. Caicedo-Reina, A. Ortiz, B. Insuasty, D. Zahn, L. Lüer and C. J. Brabec, *J. Am. Chem. Soc.*, 2025, **147**, 1957–1967.

66 T. Endale, E. Sovernigo, A. Radivo, S. Dal Zilio, A. Pozzato, T. Yohannes, L. Vaccari and M. Tormen, *Sol. Energy Mater. Sol. Cells*, 2014, **123**, 150–158.

646 | *Energy Environ. Sci.*, 2026, **19**, 635–647

This journal is © The Royal Society of Chemistry 2026

67 J. Wu, J. Zhang, L. Wang, J. Jakšić, A. Barabash, D. Veljković, A. J. Bornschlegl, V. Jovanov, L. Lahn, O. Kasian, M. E. Pérez-Ojeda, K. Götz, T. Unruh, C. Li, Z. Peng, Y. Wang, J. A. Hauch, L.-L. Deng, V. Maslak, A. Mitrović, G. Li and C. J. Brabec, *J. Am. Chem. Soc.*, 2025, **147**, 32045–32053.

68 Q. Song, V. M. Le Corre, T. Heumüller, H. Zhang, Z. Peng, A. J. Bornschlegl, X. Du, L. Lüer and C. J. Brabec, Degradation forecasting for accelerated lifetime studies in organic photovoltaics via symbolic regression, *ChemRxiv*, 2025, preprint, DOI: 10.26434/chemrxiv-2025-nkqnd.

69 J. Han, H. Xu, S. H. K. Paleti, A. Sharma and D. Baran, *Chem. Soc. Rev.*, 2024, **53**, 7426–7454.

70 J. Luke, E. J. Yang, C. Labanti, S. Y. Park and J.-S. Kim, *Nat. Rev. Mater.*, 2023, 1–14.

71 NIST XCOM: Element/Compound/Mixture, https://physics.nist.gov/PhysRefData/Xcom/html/xcom1.html, (accessed July 28, 2025).

72 H. Moriwaki, Y.-S. Tian, N. Kawashita and T. Takagi, *J. Cheminf.*, 2018, **10**, 4.

73 RDKit Release 2025.03.6 (version 2025.03.6) https://www.rdkit.org, 2025.

74 Schrödinger Release 2021-3; Maestro, Schrödinger, LLC, New York, NY (version Release 2021-3) Schrödinger, Inc., New York, NY 2021.

75 C. Liu, L. Lüer, V. M. L. Corre, K. Forberich, P. Weitz, T. Heumüller, X. Du, J. Wortmann, J. Zhang, J. Wagner, L. Ying, J. Hauch, N. Li and C. J. Brabec, *Adv. Mater.*, 2024, **36**, 2300259.

76 X. Du, L. Lüer, T. Heumueller, A. Classen, C. Liu, C. Berger, J. Wagner, V. M. Le Corre, J. Cao, Z. Xiao, L. Ding, K. Forberich, N. Li, J. Hauch and C. J. Brabec, *InfoMat*, 2024, **6**, e12554.

77 B. J. Nordell, T. D. Nguyen, A. N. Caruso, W. A. Lanford, P. Henry, H. Li, L. L. Ross, S. W. King and M. M. Paquette, *Front. Mater.*, 2019, **6**, 264.

78 J.-H. Han, S.-H. Seok, Y. H. Jin, J. Park, Y. Lee, H. U. Yeo, J.-H. Back, Y. Sim, Y. Chae, J. Wang, G.-Y. Oh, W. Lee, S. H. Park, I.-C. Bang, J. H. Kim and S.-Y. Kwon, *Nat. Commun.*, 2023, **14**, 6957.

79 D. Simeone, C. Mallet, P. Dubuisson, G. Baldinozzi, C. Gervais and J. Maquet, *J. Nucl. Mater.*, 2000, **277**, 1–10.

80 T. Stoto, L. Zuppiroli and J. Pelissier, *Radiat. Eff.*, 1985, **90**, 161–170.

81 G. J. Moore, F. Günther, K. M. Yallum, A. Causa, A. Jungbluth, J. Réhault, M. Riede, F. Ortmann and N. Banerji, *Nat. Commun.*, 2024, **15**, 9851.

82 G. U. Bublitz and S. G. Boxer, *Annu. Rev. Phys. Chem.*, 1997, **48**, 213–242.

83 V. E. Gruzdev and J. W. Arenberg, *Opt. Eng.*, 2021, **60**, 031001.

84 G. M. Lo Piccolo, M. Cannas and S. Agnello, *Materials*, 2021, **14**, 7682.

85 L. Skuja, *J. Non-Cryst. Solids*, 1998, **239**, 16–48.

86 M. Jivanescu, A. Stesmans and V. V. Afanasev, *Phys. Rev. B:Condens. Matter Mater. Phys.*, 2011, **83**, 094118.

87 M. Boero, A. Oshiyama and P. L. Silvestrelli, *Mod. Phys. Lett. B*, 2004, **18**, 707–724.

88 H. Imai, K. Arai, H. Hosono, Y. Abe, T. Arai and H. Imagawa, *Phys. Rev. B:Condens. Matter Mater. Phys.*, 1991, **44**, 4812–4818.

89 E. Yousif and R. Haddad, *SpringerPlus*, 2013, **2**, 398.

90 D. V. A. Ceretti, M. Edeleva, L. Cardon and D. R. D'hooge, *Molecules*, 2023, **28**, 2344.

91 M. Hammarson, J. R. Nilsson, S. Li, T. Beke-Somfai and J. Andréasson, *J. Phys. Chem. B*, 2013, **117**, 13561–13571.

92 X. Yu, Z. Wang, M. Buchholz, N. Füllgrabe, S. Grosjean, F. Bebensee, S. Bräse, C. Wöll and L. Heinke, *Phys. Chem. Chem. Phys.*, 2015, **17**, 22721–22725.

93 M. Poutanen, Z. Ahmed, L. Rautkari, O. Ikkala and A. Priimagi, *ACS Macro Lett.*, 2018, **7**, 381–386.

94 M. S. Jahan, J. C. Stovall, D. R. Ermer, D. W. Cooke and B. L. Bennett, *Radiat. Phys. Chem.*, 1993, **41**, 77–83.

95 J. S. Wallace, M. B. Sinclair, K. T. Gillen and R. L. Clough, *Radiat. Phys. Chem.*, 1993, **41**, 85–100.

This journal is © The Royal Society of Chemistry 2026

Energy Environ. Sci., 2026, **19**, 635–647 | **647**